

## Development of Polylactide Open-Cell Foams with Bimodal Structure for High-Acoustic Absorption

Shahrzad Ghaffari Mosanenzadeh,<sup>1</sup> Hani E. Naguib,<sup>1</sup> Chul B. Park,<sup>1</sup> Nouredine Atalla<sup>2</sup>

<sup>1</sup>Department of Mechanical and Industrial Engineering, University of Toronto, Toronto, Canada

<sup>2</sup>Groupe d'Acoustique de l'Université de Sherbrooke, Sherbrooke (GAUS), Quebec, Canada

Correspondence to: H. E. Naguib (naguib@mie.utoronto.ca).

**ABSTRACT:** In this study, a highly porous and interconnected foam structure was fabricated using compression molding combined with particulate-leaching technique. The foamed structures were fabricated with polylactide (PLA) and polyethylene glycol (PEG) with salt as the particulate. The pore size of the foam structure is controlled by the particulates size and higher interconnectivity is achieved by the co-continuous blending morphology of the PLA matrix with the water-soluble PEG. PLA is a fully bio-based thermoplastic polymer and is derived from renewable resources, such as cornstarch or sugarcane. PEG is also fully biodegradable polymer produced from ethylene. Fabricated foams were characterized for cellular, acoustic, and mechanical properties. The acoustic performance of the foams was studied by measuring the normal incident absorption coefficient in accordance with the ASTM E1050 standard. The results show open porosity as high as 88% was achieved and the effect of water-soluble polymer on cellular properties and acoustic and mechanical performance of the foams was studied. As a result of the secondary porous structure formed into cell walls by water soluble polymer, the overall absorption of fabricated PLA foams was increased to above 90% while the average absorption of the foams remained unchanged. In addition, the resulting acoustic foams are benign and environmentally friendly. © 2013 Wiley Periodicals, Inc. *J. Appl. Polym. Sci.* **2014**, *131*, 39518.

**KEYWORDS:** biopolymers and renewable polymers; foams; porous materials; properties and characterization; structure-property relations, acoustic properties, bimodal structure

Received 8 January 2013; accepted 2 May 2013

DOI: 10.1002/app.39518

### INTRODUCTION

Open-cell foams have the capability to damp acoustic energy by allowing fluid to flow through the cells and dissipate its energy. Such structures are also lightweight and are widely used as sound absorbers. Although such foams are good absorbers at higher frequencies with absorption coefficients above 0.95, they show limited acoustic absorption at lower frequencies. Another issue is that the existing foams are fabricated from petroleum-based polymers. In the case of cross-linked polymer chains, the resulting foams will be nonrecyclable and therefore will be land-filled after their end of life. On the other hand, the recyclable foams such as polypropylene foams are often too expensive to recycle and even without considering the carbon dioxide generation from recycling operation in an incineration plant, there is no economic interest in reusing these foams. The solution is to fabricate open-cell foams from bio-based polymers for noise control applications. Bio-based polymers are fabricated from renewable resources such as plants and microorganisms, these polymers break down into water, carbon dioxide, and biomass in contact with heat and humidity.

Poly(lactic acid) (PLA) is a thermoplastic polyester synthesized by fermenting the raw plant material that has been fixed inside the living plants by photosynthesis. Because it is derived from plants, it can be produced using small amounts of fossil fuel. In recent years, the interest in bio-based polymers has increased and PLA has found numerous applications in different industries. PLA possesses properties that lie between those of polystyrene (PS) and polyethylene terephthalate (PET)<sup>1</sup> and, as a bio-based alternative, it is expected to replace these commodity polymers. Its production cost is expected to decrease further as the markets for the material expand.

In a previous study,<sup>2</sup> acoustic performance of PLA open-cell foams fabricated by particulate leaching was compared with existing Polyurethane (PU) open-cell foam currently used for sound absorption. Fabricated PLA foams showed better acoustic performance at lower frequencies and higher average absorption than PU foams, but the overall acoustic performance of PLA foams needs to be improved. To improve acoustic absorption of PLA foams while also studying the relation between cell morphology and acoustic properties of polymeric open-cell foams,

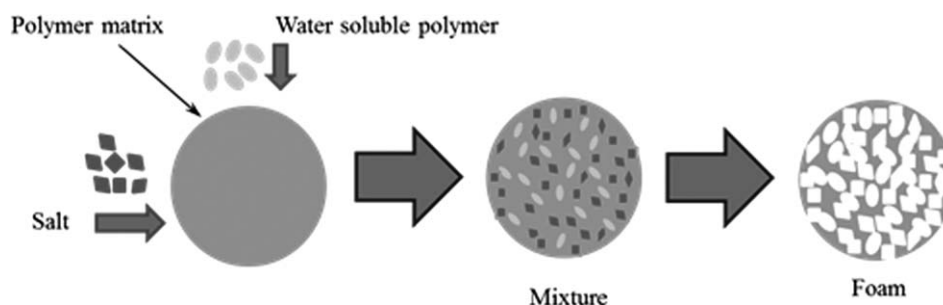


**Figure 1.** Schematic of particulate-leaching technique. [Color figure can be viewed in the online issue, which is available at [wileyonlinelibrary.com](http://wileyonlinelibrary.com)].

water-soluble polymers were used to decrease flow resistivity and hence improve the acoustic absorption of these foams. Salt and water-soluble polymers were used as the particulates in the polymer matrix. The idea is to form the larger cell structure with leaching out the salt particles while leaching the water-soluble polymer creates additional micro voids in the foam matrix resulting in a bimodal foam structure. Different weight percentages of water-soluble polymer were examined for two different amounts of PLA. The water-soluble polymer used in this study is low-molecular-weight-polyethylene glycol (PEG). Bio-based foams fabricated through this study have the potential to replace the current petrochemical-based foams.

## BACKGROUND AND LITERATURE SURVEY

There are several methods to fabricate open-cell structures for noise control including polymer expansion with pressurized gas and chemical blowing agents, emulsion freeze drying, thermally induced phase separation (TIPS), particulate leaching/solvent casting, and 3D printing technique.<sup>3–8</sup> One relatively new method for open-cell foaming is particulate leaching or salt leaching. This method involves the addition of an inhomogeneous domain into the polymer matrix at the beginning. Solid particles, such as sodium chloride and potassium chloride crystals, are introduced into the polymer matrix at the beginning of the process. These particles will later be dissolved out of the matrix by a solvent, thereby resulting in a porous cellular network throughout the entire polymer matrix.<sup>9</sup> This technology has been commonly used in the production of highly porous bio-scaffolds.<sup>10</sup> Recent research has tried to apply the particulate-leaching technique to noncontinuous batch-foaming processes. The incorporation of this technique into the rotational foam molding process has also been investigated in the literature.<sup>11,12</sup>

As a sound wave travels through an open-cell structure, its energy is absorbed by several dissipative processes such as viscous and thermal effects as well as structural vibration in case of elastic frames. In this study, the effect of a double-porosity medium on acoustic and nonacoustic properties will be investigated. The idea is to form a microporous structure in the foam matrix. Therefore, while the larger cells allow the sound wave to enter the foam, the secondary porous structure in the cell walls increases the damping effect of the overall frame. Such a structure is called bimodal for having two porous modes.

To fabricate a bimodal structure with particulate leaching method, water-soluble polymer can be used to form the

microporous structure in addition to the main porous frame formed by larger particulates. Water-soluble polymers are widely used to make highly porous scaffolds for tissue engineering purposes.<sup>13,14</sup> Pertinent methods generally use solvents, particulate leaching, co-continuous blends (water-soluble polymers), gas foaming, or some combination of these. Kramschuster and Turng<sup>15</sup> used PLA and polyvinyl alcohol (PVOH) with salt as the particulate and gas foaming with carbon dioxide to fabricate bio-based scaffolds. Kim et al.<sup>16</sup> fabricated polymeric membrane with a fine porous structure from PS, PEG, and solvent solutions by exploiting the phase separation induced in the course of dry casting. In this study, PEG was used to fabricate highly porous open-cell foams for the first time to study the effect of bimodal structures on sound absorption of PLA foams.

Another aspect of this study is to improve the knowledge on the relation between cell morphology and acoustic properties of open-cell foams. To be able to control cell structure of the foams, particulate leaching combined with compression molding was used to fabricate open-cell foams. In this fabrication method, salt and water-soluble polymer were used as leachable particulates. This fabrication method provides the possibility of monitoring cellular properties of the foam closely by changing fabrication parameters and therefore it is suitable for investigating the cell structure of the foams.

## Fabrication of PLA Open-Cell Foams

Fabrication process used in this study is the combination of particulate-leaching technique and compression-molding method.<sup>2</sup> Figure 1 shows the schematic of particulate-leaching technique. This is an ideal approach to investigate the effect of fabrication parameters on acoustic performance of the resulting open-cell foams. In this fabrication method, PLA, PEG, and salt blend is transferred into a compression molder and heated to 180°C for 10 min. Then the sample is compressed at 15 MPa for an additional 10 min. Afterwards, the dye is cooled to room temperature to remove samples. The samples will then be leached in water for 72 h. The water should be changed frequently to avoid saturation. The final stage is drying the sample in 35°C for 24 h. The geometry of samples is cylindrical with approximately 10 mm in thickness and 29 mm in diameter.

Because the melt temperature of salt is above the molding temperature, it does not melt during molding process. PEG on the other hand, melts at relatively low temperatures and therefore bonds with PLA matrix during the fabrication process. To make

**Table I.** Composition (wt %) of Foams with 10% and 15% PLA

Material composition (wt %)								
10% PLA				15% PLA				
PEG	0%	1%	2%	3%	0%	1.5%	3%	4.5%
Salt	90%	89%	88%	87%	85%	83.5%	82%	80.5%

sure that all the salt is leached silver nitrate ( $\text{AgNO}_3$ ) solution was used to evaluate the leaching procedure. If water contains a Cl ion, a white residue will be generated in the presence of an  $\text{Ag}^+$  ion. Thus, if no white residue was observed when the  $\text{AgNO}_3$  solution was dropped into the leaching solution sample, the foam samples can be considered to be completely leached. To insure that all the salt was leached out of the foam samples, the samples were weighted before leaching and after drying. The final sample weight has to be less than the weight of the polymer used to fabricate the foam.

In order to study the effect of water-soluble polymer on cellular structure and consequently the acoustic performance of the resulting foams, different amounts of water-soluble polymer were compared while keeping the weight percent of the PLA constant. For PLA containing 10% and 15% of the total weight of the material, PEG to PLA weight ratios of 0, 0.1, 0.2, and 0.3 were examined, we will refer to these combinations as foams with 0%, 10%, 20%, and 30% PEG through this article. Table I shows the weight percentage of PLA, PEG, and salt used for different foam samples. Fabricated foams were characterized in terms of their cellular, mechanical, and acoustic properties.

## EXPERIMENT

### Experimental Material

Two bio-based polymers were used to fabricate foam samples. PLA is a bio-based thermoplastic polymer, which is derived from renewable resources, such as cornstarch or sugarcanes. The PLA powder used in this study was provided by ICO Polymers. The powder has spherical particles, which are 20  $\mu\text{m}$  in diameter. The density of PLA is 1.24  $\text{g}/\text{cm}^3$ , melt flow index is 15  $\text{g}/10$  min, glass-transition temperature is 60°C, and its melt temperature is 150°C.

PEG is a bio-based water-soluble polymer. PEG was manufactured by Wako Pure Chemical Industries, Ltd. Melt temperature of PEG is around 30°C and the molecular weight of PEG is approximately 2000. PEG was in the form of platelets, which was grinded by mortar and pestle and the PEG powder was then sieved to less than 250  $\mu\text{m}$ . Salt used in this study was commercially available sodium chloride. The salt particles were cubic and were sieved into 250–500  $\mu\text{m}$ .

## CHARACTERIZATION METHODS AND MEASURED PROPERTIES

In order to characterize fabricated foam samples, different thermal (differential scanning calorimetry, cellular (porosity, average pore size, and cell density), mechanical (yield stress and elastic modulus), and acoustic (sound absorption coefficient and static airflow resistivity) properties were measured.

## Thermal Properties

Thermal characteristics of PLA and PEG were determined by differential scanning calorimetry (DSC 2000, TA Instruments) using a heat-cool-heat cycle between 10°C and 200°C with a heating and cooling rate of 5°C/min.

Differential scanning calorimetry (DSC) is a thermal analysis technique used to determine the glass-transition temperature ( $T_g$ ), crystallization temperature ( $T_c$ ), melting temperature ( $T_m$ ), and the enthalpies associated with the crystallization and melting. It can also be used to measure the percent of crystallinity within the sample. The DSC system measures the difference in the heat required to increase the temperature of a sample and a reference as a function of temperature. The reference is an empty aluminum pan. The temperatures of the empty pan and a pan containing sample are kept identical to one another by controlling the amount of heat flowing into each system to maintain a constant heating or cooling rate. When the temperature at which a phase transition occurs for a particular material, a peak will be observed on the thermograph. Glass-transition points, melting temperatures, and degree of crystallinity were determined for PLA, PEG, and blends of the two polymers from the thermograms.

Enthalpies of these processes can be calculated by measuring the area under the peaks to determine the percent crystallinity of the sample using eq. (1)<sup>17,18</sup>:

$$\% \text{Crystallinity} = \frac{\Delta H_m - \Delta H_c}{\Delta H_m^0} \times 100\% \quad (1)$$

where  $\Delta H_m$  is the heat of melting,  $\Delta H_c$  is the heat of cold crystallization, and  $\Delta H_m^0$  is a reference value which represents the heat of melting if the polymer was 100% crystalline. The degree of crystallinity is one of the most important properties of a polymer sample because it influences all the mechanical properties such as tensile strength, modulus, elongation, and impact strength.<sup>19</sup> Reference melt enthalpies for 100% crystalline PLA of 93.7  $\text{J}/\text{g}$ <sup>20</sup> and PEG of 202.41  $\text{J}/\text{g}$ <sup>21</sup> are used to calculate the percent of crystallinity.

Thermogravimetric analysis (TGA) was also performed for pure PLA and PEG as well as different PLA-PEG blends. TGA measures the amount and rate of change in the weight of a material as a function of temperature or time in a controlled atmosphere. TGA was performed by TGA Q 50 from TA instruments. The sample was heated from room temperature to 600°C using the temperature ramp at 20°C/min under nitrogen.<sup>22</sup>

## Cell Morphology

Cell morphology of foam samples was examined using images obtained from a JEOL JSM 6060 scanning electron microscope (SEM) and the ImageJ software. Samples were frozen in liquid nitrogen and fractured to obtain a clean cross section, sputter coated with platinum, and micrographs were taken in the SEM. The fractured surface was examined at multiple regions for irregularities in the cellular structure. The average of approximately 20 pores was taken as the average cell size for each set of foam samples. Cell density of the samples was estimated using the following correlation:

$$\text{Cell density} = \left( \frac{\text{Number of cells}}{\text{Area}} \right)^{3/2} \cdot \frac{\text{Bulk density}}{\text{Foam density}} \quad (2)$$

### Physical Properties

Porosity and airflow resistivity are two of the most important macroscopic properties, which directly influence the acoustic behavior of a medium. The open-cell content of a foam material is the percentage of the material that is interconnected with the ambient environment. Porosity of foam samples was measured by a gas pycnometer (Quantachrome Instrument Ultra-Foam 1000) in accordance with the ASTM D6226 standard. The pycnometer pressurizes the foam sample with nitrogen at 6 psi and measures the closed volume that cannot be penetrated by the pressurized nitrogen,  $V_{\text{closed}}$ . The open-cell content,  $\phi_v$ , is measured using the following equation where  $V_{\text{geometric}}$  is the geometric volume of the sample. Results were averaged between three or more specimens from each set of foam samples.

$$\Phi_v = \left( 1 - \frac{V_{\text{closed}}}{V_{\text{geometric}}} \right) \times 100\% \quad (3)$$

Another measured macroscopic property is static flow resistivity, which greatly influences the acoustic behavior of a material. Static airflow resistivity is defined as airflow resistance per unit thickness of the material. The static airflow resistivity was measured according to the ASTM C522 standard. Airflow rate ( $U$ ) and pressure difference across the sample ( $P$ ) are measured by airflow resistivity meter and the airflow resistivity ( $\sigma$ ) can be calculated from eq. (4). Here,  $A$  is the cross-sectional area and  $t$  is the thickness of the sample. During tests foam samples were sealed with Teflon tape to avoid air leakage at edges.

$$\sigma = \left( \frac{P \times A}{U \times t} \right) \quad (4)$$

### Mechanical Properties

Mechanical performance of foam samples was measured through compression test performed by Instron 5548 500N micro tester according to ASTM D1621. Three samples were tested for each category and values of Young's modulus and yield stress were derived from stress-strain curves. During testing, samples were preloaded to 5 N and the strain rate was 1 mm/min.

### Acoustic Properties

Fabricated foams were characterized based on their capability for acoustic absorption. Sound absorption coefficient ( $\alpha$ ) of a material is the amount of sound energy that can be absorbed by that material and can take values from 0 to 1. Where 1 represents total absorption and 0 represents total reflection. The ability of foam samples to absorb sound energy was measured by impedance tube based on two-microphone transfer function method in accordance with the ASTM E1050 standard. In the two-microphone transfer function method, a loudspeaker is mounted at one end of an impedance tube and a small sample of the material (a 29 mm in diameter cylinder) is placed at the other end. Figure 2 shows a schematic of the impedance tube. In Figure 2,  $P_I$  and  $P_R$  represent the incident and reflected wave pressures.  $P_1$  and  $P_2$  are the two microphones placed at  $X_1$  and  $X_2$  distances from the foam sample. The loudspeaker generates broadband, stationary random sound waves. These propagate as plane waves in the tube, hit the sample and are reflected resulting in a

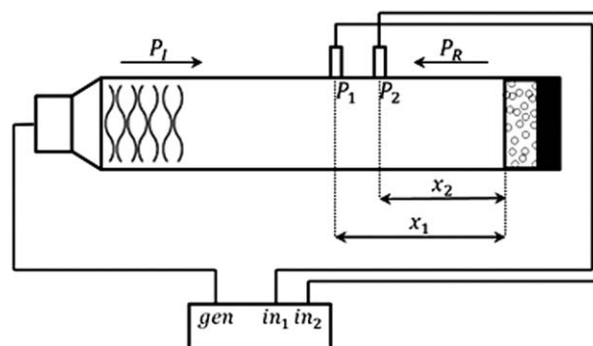


Figure 2. Schematic of two-microphone impedance tube.

standing wave interference pattern. The sound pressure at two locations is measured and the complex transfer function calculated. It is then possible to determine the complex reflection coefficient, the sound absorption coefficient, and the normal acoustic impedance of the material. Diameter of impedance tube is 29 mm with frequency range of 800–6300 Hz.

## RESULTS AND DISCUSSION

### Thermal Properties

The DSC heating and cooling thermograms for PEG and PLA are shown in Figure 3. On the heating curve of PLA, at the glass-transition temperature a shift down in the baseline occurs, indicating that heat is being added to the sample to move through the transition and an endothermic process is taking place. Glass-transition temperature of PLA was measured to be 59.45°C. As the temperature is increased, an upward peak appears on the thermograph, which indicates that an exothermic process takes place whereby less heat is required to raise the sample temperature. This is referred to as cold crystallization. By further increasing the temperature at the melt point of the material, more heat flow is required to increase the temperature of the sample at the same rate as the reference and a downward peak appears on the thermograph, indicating an endothermic process. The melt temperature of PLA was measured to be 139.80°C. Degree of crystallinity of PLA during the second heating cycle was measured to be 17.24% based on DSC results.

For PEG, the melt temperature was 53.14°C from DSC results and the degree of crystallinity was measured to be 89.13%.

For blends of PLA and PEG, as the amount of PEG is increased the shift down in the heating curve at 140°C decreases and in return a shift down at around 50°C appears for 20% PEG and 80% PLA and further increases by increasing the PEG content. On the cooling thermograms, by increasing the PEG content a crystalline exothermic peak appears during this cycle.

TGA results are shown in Figure 4. Neat PLA undergoes one-stage decomposition at 375°C with no residuals remaining at 600°C and PEG undergoes one-stage decomposition at 446°C with no residuals remaining at 600°C. Both thermal degradation temperature and thermal degradation rate decrease by increasing the amount of PEG in the PLA-PEG blend. All blends exhibit a two-stage decomposition, which is because of separate



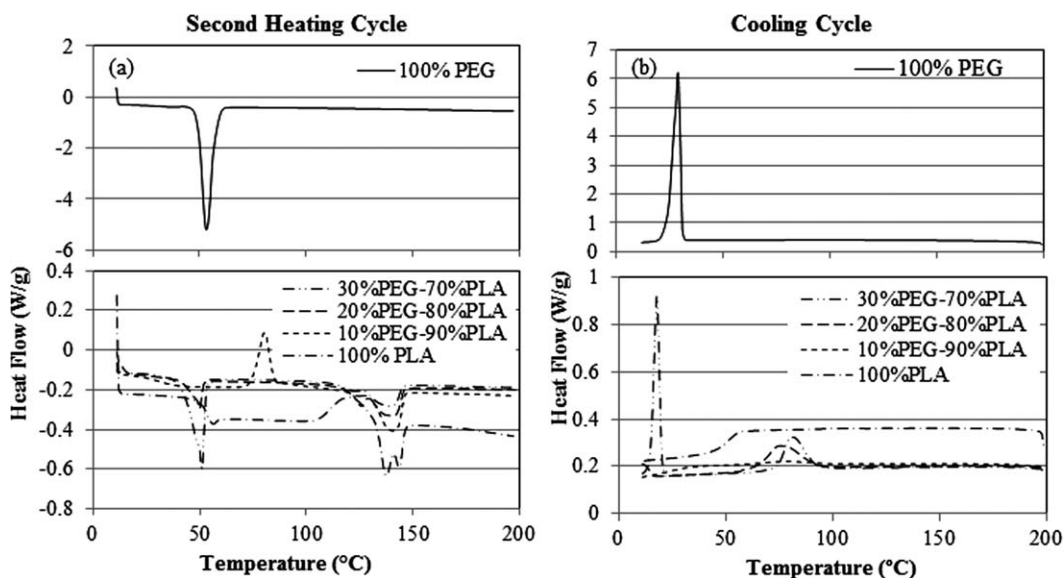


Figure 3. DSC thermograms for PLA and PEG for (a) heating and (b) cooling processes.

PLA and PEG phases. The results suggest that the first degradation step is because of the PLA fraction and the second is because of the PEG portion. Even though the degradation temperature of PEG is higher than PLA, by increasing the PEG content, decomposition temperature of the blend decreases. This is because of the penetration of PEG into the PLA matrix, which forms cracks after cooling the sample because of the difference in thermal expansion of the two polymers. These opening in the PLA matrix increase the interface area and facilitate heat and mass transfer through the polymer blend. Figure 5 shows the SEM micrographs of PLA–PEG blends with 200 and 1000 magnification and electron voltage of 20 kV. The PLA powder has average particle size of 20  $\mu\text{m}$ . When blending PLA and PEG, PEG fills the gaps between PLA particles in liquid phase, resulting in cracks and microsize openings in the solidified blend. As is evident in the SEM micrographs, by increasing the amount of PEG from 10% to 20%, more cracks are formed in the PLA matrix. When increasing the temperature during the TGA test, PEG melts at 50°C making openings throughout the blend, which can result in decreasing the degradation temperature by two mechanisms. First, the openings increase heat transfer into the sample making it possible to heat up the PLA matrix from different angles. Second, the cracks increase the mass transfer in the blend and the by-products of degradation can leave the sample in less time. As the amount of PEG in the blend is increased to 30%, PLA particles are covered with PEG seen in the SEM image as individual spherical elements rather than a uniform PLA matrix, further increasing the heat and mass transfer between the PLA particles.

There was no detectable residual left at 600°C for PLA–PEG blends. DSC and TGA tests were performed on three samples from each category and the results were averaged. The average deviation of the DSC results was 6% and for TGA results was 0.1%.

#### Cell Morphology of PLA Foams

Cellular structure of porous medium is responsible for the resulting macroscopic properties measured in terms of acoustic,

thermal, and electrical parameters. In the case of sound absorption in particular, cellular structure of porous medium is responsible for the resulting macroscopic properties measured in terms of acoustic, thermal, and electrical parameters. In the case of sound absorption in particular, cell geometry, cell size, size, and shape of openings between cells and cell wall thickness are some of the most influential structural characteristics that control the maximum amount of sound absorption as well as the frequency of the maximum absorption. For example, as the frequency of sound wave decreases, wavelength increases, therefore the size of the pores in the porous medium must be proportional to the wavelength of the intended frequency range to reach the optimum sound absorption. Acoustic capability of a porous medium is directly related to fluid flow through the medium, which is affected by the volume and shape of the pore structure. The quantity of void space is referred to as porosity represented by  $\phi$ , which is the ratio of permeable volume to the overall volume of the porous medium. The actual microscopic fluid path through the void space is quantified by tortuosity. Tortuosity is a measure of the complexity of fluid path inside the porous structure denoted by  $\alpha_{\infty}$ . As the fluid path

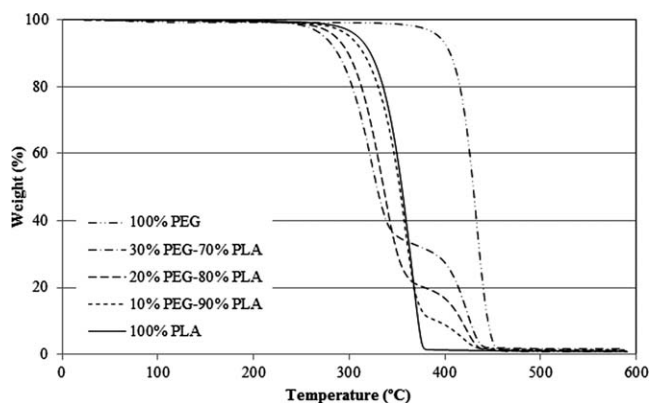


Figure 4. TGA thermograms for PLA and PEG.

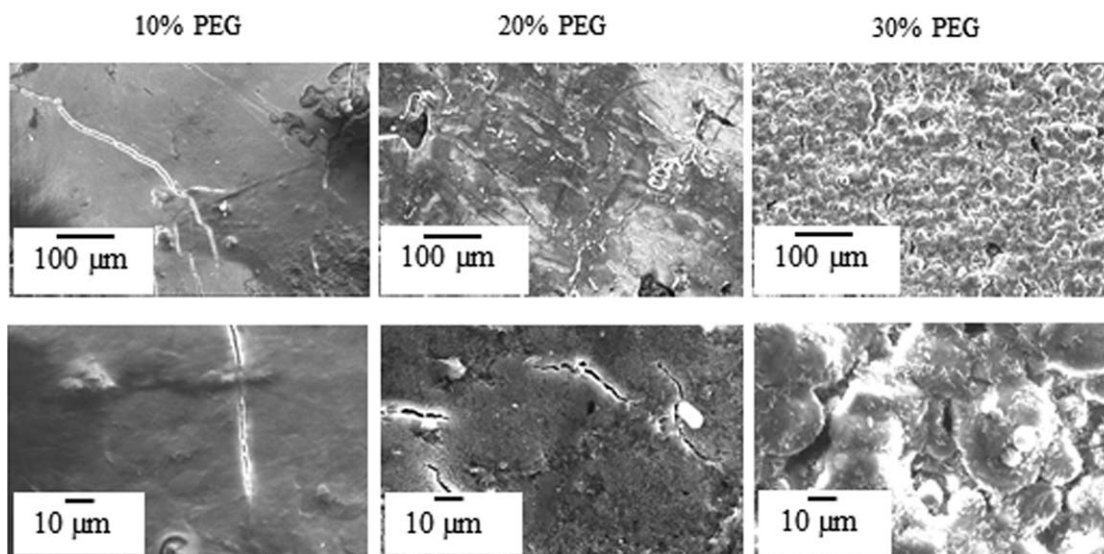


Figure 5. SEM micrographs of PLA-PEG blends with 10%, 20%, and 30% PEG.

becomes more complicated, tortuosity increases which in turn results in higher resistance to fluid flow ( $\sigma$ ). Tortuosity directly influences propagation of acoustic waves, heat and electric conductivity, filtration, and absorbance efficiency of porous mediums. Figure 6 shows a schematic demonstrating the effect of microstructure on porosity, tortuosity, and flow resistivity of a porous medium. The main cell structure of the foams fabricated through this study is formed by dissolving the salt particles, which results in the cubic shape cells. While the cells in chemically foamed structures have complicated tetrakaidecahedral geometries, the simpler cubic cell structure of the presented PLA foams, makes these foams an ideal case for studying the relation between micro- and macroproperties of open-cell structures. Figure 7 shows the PLA foam samples fabricated with 10% [Fig. 7(a)] and 15% [Fig. 7(b)] polymer and different PEG contents. Samples have cylindrical geometry to fit the impedance tube for acoustic test. Cellular structure of the foam samples was studied by SEM. Figure 8(a) shows the cell morphology of foam samples with 10 wt % PLA and increasing amount of water-soluble polymer from 0% to 30% from left to right. The magnification of SEM micrographs in Figure 8 is 100 and electron voltage is 20 kV. Micropores were observed in SEM images of the foams with different amounts of water-soluble polymer. Because PEG melts during the molding

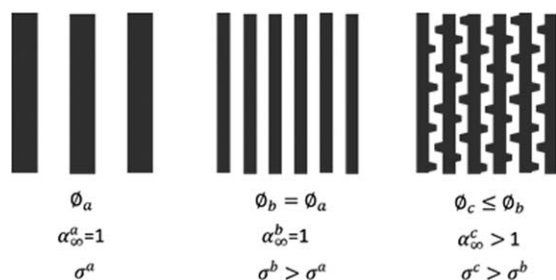


Figure 6. Schematic of the effect of fluid path through a porous medium on porosity, tortuosity, and flow resistivity.

process, it blends with the melted PLA. The PEG powder was sieved to less than 250  $\mu\text{m}$  and leaching out the PEG leaves micropores and cracks inside the PLA matrix. As observed from SEM images, cells have cubic shape, which is because of the shape of salt particles. Figure 8(b) shows the cell morphology of foam samples with 15 wt % PLA and different amount of water-soluble polymer. As seen in images, by increasing the amount of PEG, the cracks in the cell structure increases.

Cellular properties of samples such as cell density and average cell size were estimated from SEM images. The foam's cellular structure is created by leaching out PEG and salt particles, therefore, as the polymer mass ratio decreases from 15% to 10%, the number of cells and consequently the cell density increases. Average cell size on the other hand, remains constant and close to average salt particle size, respectively. Adding PEG does not show any considerable effect on cell density and cell density for foams with 15% PLA was approximately  $11 \times 10^4$  cells/cm<sup>3</sup> and for foams with 10% PLA was approximately  $20 \times 10^4$  cells/cm<sup>3</sup>. Average cell size for all foam samples was in the range of 350  $\mu\text{m}$ .

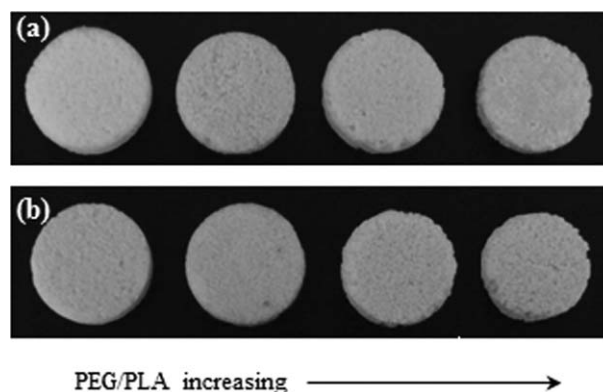


Figure 7. Image of foam samples with (a) 10% PLA and (b) 15% PLA for PEG/PLA equal to 0, 0.1, 0.2, and 0.3. [Color figure can be viewed in the online issue, which is available at wileyonlinelibrary.com].

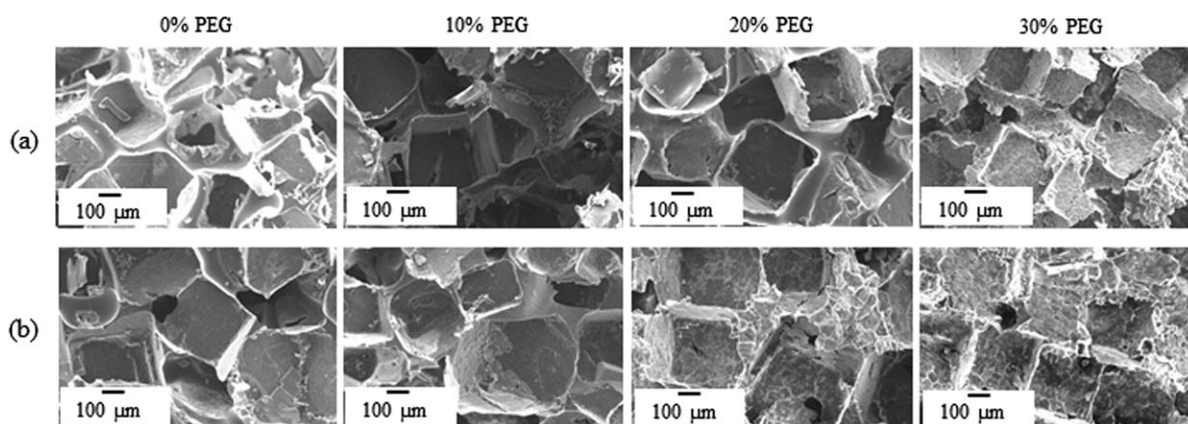


Figure 8. SEM micrographs of foams with (a) 10% PLA and (b) 15% PLA for 0%, 10%, 20% and 30% PEG.

SEM images of PLA foam samples with magnification of 1000 and electron voltage of 20 kV are shown in Figure 9. As stated before, by increasing the PEG content, more cracks were formed in the foam structure. For foam samples with 10% PLA, as is shown in Figure 9(a), number of microvoids increases as the PEG content is increased and for PEG/PLA ratio of 0.3 micro-openings are extended all over the foam resulting in a bimodal structure. As mentioned previously, the PLA powder has the average particle size of 20  $\mu\text{m}$  and it can be seen that PEG even penetrated the PLA particles. The same trend was observed for foam samples with 15% PLA as shown in Figure 9(b).

#### Physical Properties

Open-cell structures intended for sound absorption applications must have high porosities (around 90%) to allow the sound wave to enter the damping structure and dissipate its energy while passing through the convoluted path way between the cells. One important achievement in this study is the high porosity of fabricated foam samples, porosity results are shown in Figure 10(a). As expected, open porosity increases by decreasing polymer mass ratio. Porosity for foams with 15% PLA was around 82% and for foams with 10% PLA was around 88%. On the other hand, increasing the PEG content has no

effect on the porosity. Because the scale of pores and cracks formed by water-soluble polymer is very small compared to the main pores, porosity of the foams is not affected by PEG amount.

Porosity can be also estimated by knowing the weight of the polymer used in fabricating the foam, density of the polymer, and geometrical volume of the fabricated foam sample as explained in eq. (5).

$$\begin{aligned} \text{Porosity} &= \left( 1 - \frac{\text{Polymer volume}}{\text{Foam's geometric volume}} \right) \\ &= \left( 1 - \frac{\text{Polymer mass/polymer density}}{\text{Foam volume}} \right) \end{aligned} \quad (5)$$

Foam density was measured using the density measurement kit for a Denver Instruments mass balance. The density measurement accounts for the mass of the sample in air and in water and calculates the specific gravity while correcting for the effects of the water temperature. Estimated porosities for PLA foams were 88.68% for 10% polymer and 81.8% for 15% polymer, which is close to measured values listed in Tables II and III.

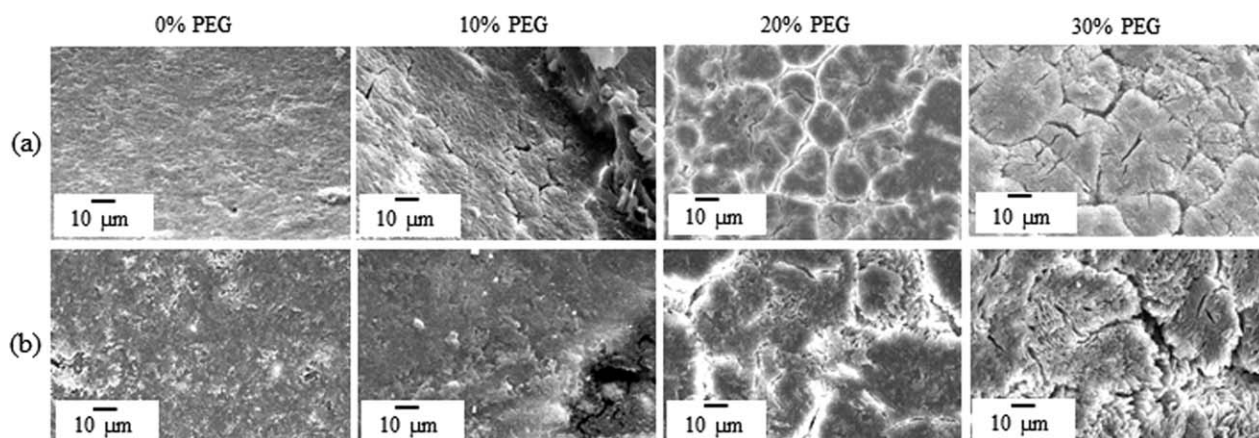
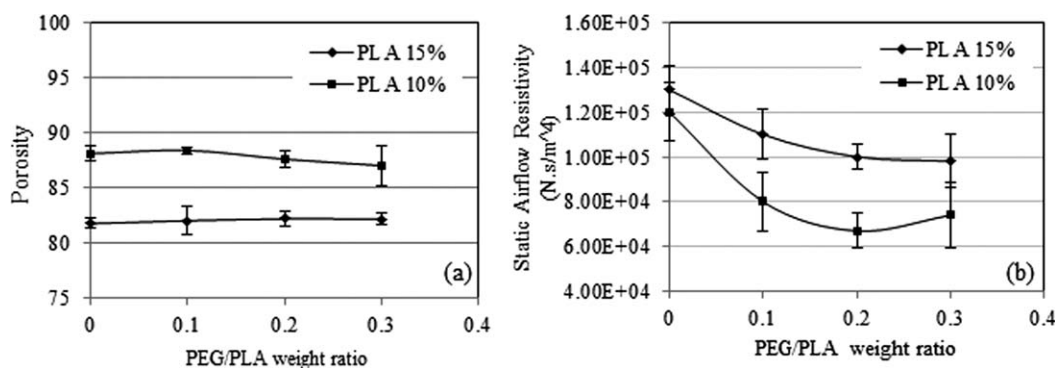


Figure 9. SEM micrographs of foams with (a) 10% PLA and (b) 15% PLA for 0%, 10%, 20% and 30% PEG.





**Figure 10.** (a) Open porosity and (b) static airflow resistivity results for PLA foams with different PEG to PLA weight ratios.

In the same category of open-cell foams, the ones with lower static airflow resistivity allow the fluid to flow through the structure more easily and therefore have higher sound absorption. Results for static airflow resistivity at 0.1 L/min flow rate are shown in Figure 10(b). As also observed in previous study,<sup>2</sup> by decreasing the PLA weight percentage, flow resistivity decreases. Also by adding the water-soluble polymer, flow resistivity decreases for both foams with 15% and 10% PLA. Flow resistivity further decreases by increasing the PEG content for foams with 15% PLA, while for foams with 10% PLA, flow resistivity shows an increase for PEG/PLA weight ratio of 0.3.

### Mechanical Properties of PLA Foams

Because the fabricated foams are proposed for acoustic applications, these foams will be used between layers of structure and are not intended to sustain any load. On the other hand, the structural strength of the foams should be enough to hold the structural integrity and withstand possible pressure or impact during fabrication or assembly. Figure 11 shows the mechanical properties of PLA foams. In general, by decreasing the amount of PLA from 15% to 10%, mechanical strength of the foam decreases. This is because of the decrease in the amount of solid polymer which forms the foam structure. By reducing solid polymer in the foam structure, cell walls become thinner and bare less compressive loads before breaking. Therefore, mechanical strength and elasticity of the foam decreases, respectively.

The values of elastic modulus and compressive load at yield stress for PLA foams are listed in Table IV. As observed from

the results, for foams with 15% PLA, compressive load at yield stress and elastic modulus decreases by increasing the amount of water-soluble polymer. This can be explained by previous observations from SEM images. Addition of water-soluble polymer results in the bimodal structure, which weakens the foam because of the formation of cracks and micropores in the cell walls.

The same trend was observed for foams with 10% PLA, although the decrease in compressive load at yield stress and elastic modulus by increasing the amount of water-soluble polymer is not as significant as it was for the samples with 15% PLA. This is because of the lower amount of polymer in the foam structure.

### Acoustic Properties of PLA Foams

Even though the formation of secondary microstructure does not affect the porosity of the PLA foams, it decreases the airflow resistivity and therefore it is expected to have a positive effect on sound absorption properties of the foams. Figure 12(a) shows the acoustic absorption results for foams with 15% PLA and PEG/PLA weight ratios of 0, 0.1, 0.2, and 0.3. The results are average of four or more samples. During the test, foam samples were sealed by Teflon tape to avoid leaks around the edges. Adding water-soluble polymer to PLA foams increases the maximum acoustic absorption coefficient and also increases the frequency of maximum acoustic absorption. This is because of the decrease in flow resistivity by making cell walls more open. Although the porosity is constant, micropores generated in the cell structure by PEG improves the acoustic absorption of the PLA foams.

**Table II.** Physical and Acoustic Properties of 10% PLA Foams

Foam material	Porosity	Flow resistivity (N.s/m <sup>4</sup> )	Average absorption coefficient	Frequency at $\alpha_{\max}$ (Hz)
PEG/PLA = 0	88.06	$1.2 \times 10^5$	0.56	2500
PEG/PLA = 0.1	88.34	$8 \times 10^4$	0.58	2800
PEG/PLA = 0.2	87.55	$6.7 \times 10^4$	0.57	3350
PEG/PLA = 0.3	86.96	$7.4 \times 10^4$	0.56	3350

**Table III.** Physical and Acoustic Properties of 15% PLA Foams

Foam material	Porosity	Flow resistivity (N.s/m <sup>4</sup> )	Average absorption coefficient	Frequency at $\alpha_{\max}$ (Hz)
PEG/PLA = 0	81.74	$1.3 \times 10^5$	0.53	1900
PEG/PLA = 0.1	82	$1.1 \times 10^5$	0.58	2370
PEG/PLA = 0.2	82.17	$1.0 \times 10^5$	0.54	2500
PEG/PLA = 0.3	82.14	$9.8 \times 10^4$	0.53	2800



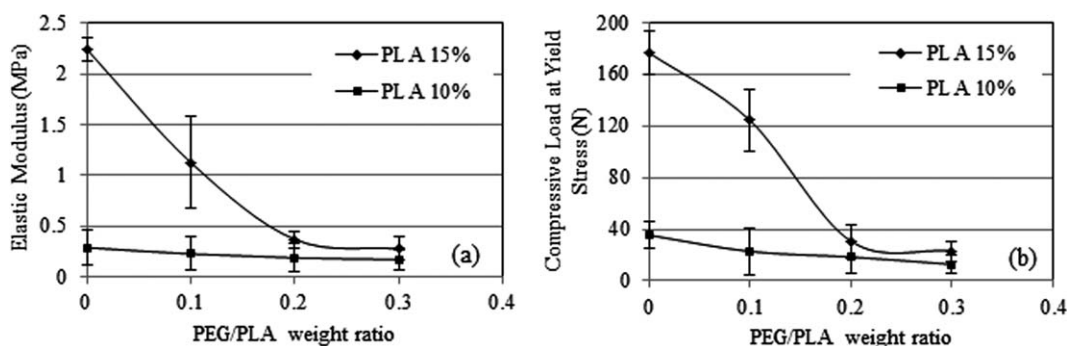


**Figure 11.** (a) Elastic modulus and (b) compressive load at yield stress of PLA foam samples with different PEG contents.

Figure 12(b) shows the acoustic absorption results for foams with 10% PLA with different PEG contents. By increasing the PEG content, the maximum absorption coefficient and the frequency of maximum absorption increases except for the case where PEG/PLA weight ratio is 0.3. It was also observed that the airflow resistivity was increased for this foam sample.

The frequency, at which the maximum absorption occurs, increases by increasing the amount of water-soluble polymer, these results are shown in Figure 13(a). To access globally the acoustic absorption performance of different materials, the average sound absorption is defined as the average of the sound absorption coefficient determined at octave bands with center frequencies 250, 500, 1000, 2000, and 4000 Hz. Average absorption coefficient determines the overall acoustic performance of the porous material and is shown in Figure 13(b). The average acoustic absorption remains relatively constant by increasing the amount of water-soluble polymer.

As mentioned before, cellular structure of open-cell foams plays the most important role in acoustic capabilities of these materials. In particular, as the cell wall thickness decreases there will be more openings between cells and hence porosity of the foam increases which in turn improves the acoustic absorption. Cell wall thickness of the foams can be measured from the SEM images. The average cell wall thickness for foams with 15% PLA is 15  $\mu\text{m}$  and for foams with 10% PLA is 9.4  $\mu\text{m}$ . As shown in Figure 9, PLA foams fabricated with less polymer have higher sound absorption for the same amount of water-soluble polymer. The down side of decreasing the amount of polymer in

the foam matrix is the loss of mechanical strength. As the cell walls become thin, the foam structure becomes weaker.

While macroscopic properties such as porosity and airflow resistivity can be determined by direct measurement techniques, microscopic cellular properties such as tortuosity, viscous and thermal characteristic lengths are very difficult to obtain because of the complexity of open-cell structures. The relation between foam morphology and acoustic properties is still an open problem in the field of acoustics. There are indirect and inverse characterization techniques to determine aforementioned cellular properties of open-cell foams, which involves modeling and simulation of the cellular structure. Experimental study of the effect of various cell structures on the resulting acoustic properties is the first step to better understand the relationship between foam structure and acoustic absorption to optimize open-cell foams for the intended applications.

## CONCLUSION

Through this study, PLA open-cell foams were fabricated with a new method to show the effect of bimodal cell structure on sound absorption of open-cell foams. The foams were characterized for different acoustic, cellular, and mechanical properties and the relation between macroscopic acoustical properties and absorption capabilities as well as mechanical strength was studied.

Particulate leaching combined with compression molding was used to fabricate open-cell foams from PLA. By adding PEG, the effect of water-soluble polymer on foam structure and acoustic behavior of PLA foams was studied. PLA weight percentages of 10 and 15 were examined with PEG/PLA weight ratios of 0, 0.1, 0.2, and 0.3.

A new bimodal structure was created as a result of leaching out the water-soluble polymer. Acoustic absorption of PLA foams was successfully improved by adding water-soluble polymer to form cracks and micropores in the cellular structure and therefore decreasing the static airflow resistivity. Because the size of the openings formed by water-soluble polymer is in the range of micron, porosity was not affected by adding water-soluble polymer. The second microstructure formed by water-soluble polymer has a positive effect on acoustic absorption of the fabricated PLA foams by decreasing the airflow resistivity, which results in improved sound absorption by increasing the

**Table IV.** Mechanical Properties of PLA Foams

PEG/PLA	10% PLA		15% PLA	
	Elastic modulus (MPa)	Compressive load at yield stress (N)	Elastic modulus (MPa)	Compressive load at yield stress (N)
0	0.29	35.5	2.243	176.9
0.1	0.23	22.8	1.126	124.4
0.2	0.19	18.5	0.370	30.8
0.3	0.17	12.7	0.276	23.1

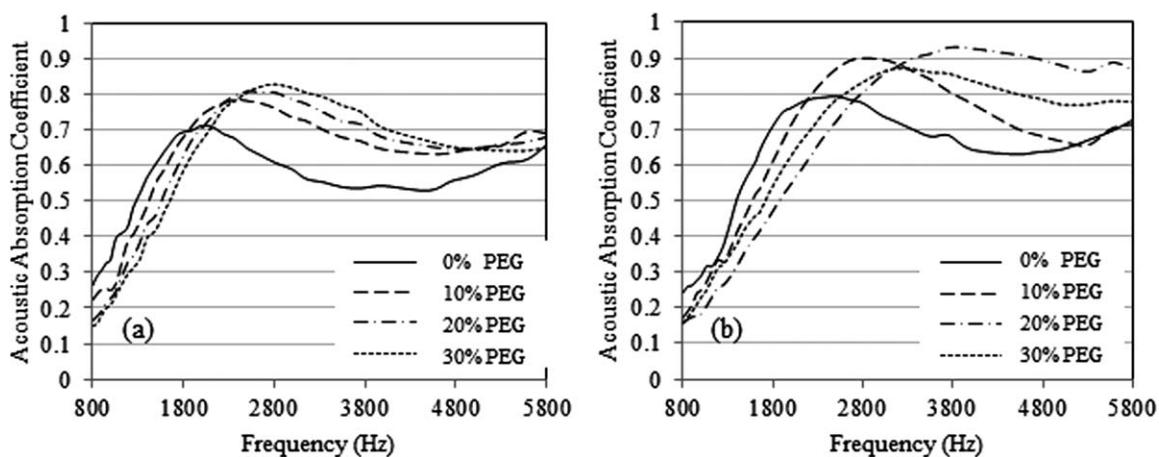


Figure 12. Sound absorption coefficient vs. frequency for foams with (a) 15% PLA and (b) 10% PLA.

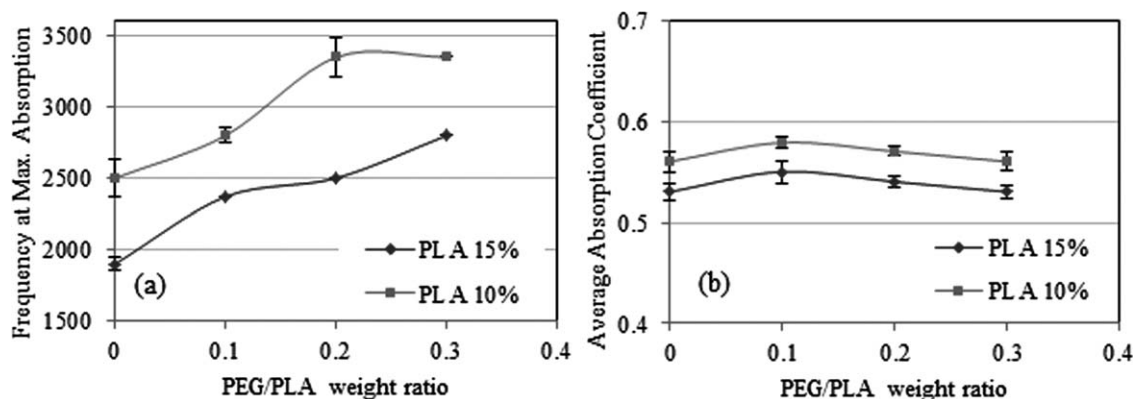


Figure 13. (a) Frequency at maximum absorption coefficient and (b) average absorption coefficient of PLA foams with different PEG to PLA weight ratios. [Color figure can be viewed in the online issue, which is available at wileyonlinelibrary.com].

maximum absorption coefficient. While the addition of water-soluble polymer increases maximum absorption coefficient and the peak frequency, it does not have any considerable effect on average absorption coefficient.

Addition of PEG to PLA foams had a negative effect on mechanical properties of the foams. Mechanical strength of the foams decreases by adding water-soluble polymer. Because of the micropores formed in the cell walls of the foams, both compressive load at yield stress and elastic modulus decreases by increasing the amount of water-soluble polymer, the decrease of mechanical properties is more noticeable in case of foams with 15% PLA. Because the application of these foams is as sound absorbers in which they do not require high-mechanical strength and load-bearing capabilities, foams fabricated through this study have a promising potential to replace the existing petrochemical-based foams. In addition, fabricated PLA foams are bio-based which resolves the environmental concerns regarding landfilling or even recycling the foams after their end of life.

#### ACKNOWLEDGMENTS

The authors acknowledge the financial support from the Natural Sciences and Engineering Research Council (NSERC) of Canada,

the Canada Research Chairs Program, and the Canada Foundation of Innovation.

#### REFERENCES

- Bohlmann, G. M. In *Handbook of Bio-Based Polymers*; Bastioli, C., Ed.; Rapra Technology: Shawbury, **2005**; p 183.
- Ghaffari Mosanenzadeh, S.; Naguib, H. E.; Park, C. B.; Atalla, N. *J. Polym. Eng. Sci.* **2013**, DOI 10.1002/pen.23443.
- Mikos, A. G.; Thorsen, A. J.; Czerwonka, L. A.; Bao, Y.; Langer, R.; Winslow, D. N.; Vacanti, J. P. *Polymer* **1994**, *35*, 1068.
- Nam, Y. S.; Yoon, J. J.; Park, T. G. *J. Biomed. Mater. Res.* **2000**, *53*, 1.
- Lo, H.; Kadiyala, S.; Guggino, S. E.; Leong, K. W. *J. Biomed. Mater. Res.*, **1998**, *30*, 475.
- Nam, Y. S.; Park, T. G. *J. Biomed. Mater. Res.* **1999**, *47*, 8.
- Lee, P. C.; Naguib, H. E.; Park, C. B.; Wang, J. *Polym. Eng. Sci.* **2005**, *45*, 1445.
- Fossey D. J.; Smith, C. H. *J. Cellular Plastics* **1973**, *9*, 268.
- Oh, S. H.; Kang, S. G.; Kim, E. S.; Cho, S. H.; Lee, J. H. *Biomaterials* **2003**, *24*, 4011.

10. Lee, P. C.; Li, G.; Lee, J. W. S.; Park, C. B. *J. Cellular Plastics* **2007**, *43*, 431.
11. Chu, R. K. M.; Naguib H. E.; Atalla, N. *SPE-ANTEC Tech. Papers*, **2008**.
12. Chu, R. K. M.; Naguib, H. E.; Atalla, N. *J. Polym. Eng. Sci.* **2009**, *49*, 1744.
13. Yang, S.; Leong, K.; Du, Z.; Chua, C. *J. Tissue Eng.* **2001**, *7*, 679.
14. Okaji, R.; Sakashita, S.; Tazumi, K.; Taki, K.; Nagamine, S.; Ohshima, M. *J. Mater. Sci.* **2012**, DOI 10.1007/s10853-012-6973-2.
15. Kramschuster, A.; Turng, L. *J. Biomed. Mater. Res. Part B Appl. Biomater.* **2010**, *92B*, 366.
16. Kim, J.; Taki, K.; Nagamine, S.; Ohshima, M. *J. Appl. Polym. Sci.* **2009**, *111*, 2518.
17. Gray, A. P. *J. Thermochim. Acta* **1970**, *1*, 563.
18. Richardson, M. J. *J. Polym. Sci. Part C Polym. Symp.* **1972**, *38*, 251.
19. Sperling, L. H. *Introduction to Physical Polymer Science*, 4th ed.; John Wiley and Sons: Hoboken, NJ, **2006**.
20. Smith, P.; Lemstra, P. J.; Booiij, H. C. *J. Polym. Sci. Polym. Phys.* **1981**, *19*, 877.
21. Joykumar Singh, T. H.; Bhat, S. V. *Bull. Mater. Sci.* **2003**, *26*, 707.
22. D'Antone, S.; Bignotti, F.; Sartore, L.; D'Amore, A.; Spagnoli, G.; Penco, M. *J. Polym Degrad. Stability* **2001**, *74*, 119.
23. Ishizaki, K.; Komarneni, S.; Nanko, M. *Porous Materials Process Technology and Applications*; Kluwer Academic Publishers: the Netherlands, **1998**.
24. Mikos, A. G.; Thorsen, A. J.; Czerwonka, L. A.; Bao, Y.; Langer, R.; Winslow, D. N.; Vacanti, J. P. *Polymer*, **1994**, *35*, 1068.
25. Nam, Y. S.; Yoon, J. J.; Park, T. G. *J. Biomed. Mater. Res.* **2000**, *53*, 1.
26. Lo, H.; Kadiyala, S.; Guggino, S. E.; Leong, K. W. *J. Biomed. Mater. Res.* **1998**, *30*, 475.
27. Allard, J. F.; Atalla, N. *Propagation of Sound in Porous Media—Modeling Sound Absorbing Materials*, 2nd ed.; Wiley: New York, **2009**.